Journal of Materials Science Research and Reviews

Volume 10, Issue 4, Page 8-15, 2022; Article no.JMSRR.95374

Synthesis and Characterization of Zinc Oxide (ZnO) Thin Films for Solar Cell Applications Using Sol-Gel Auto Combustion Technique

S. M. Kurawa [a*], A. O. Musa [b], T. H. Darma [b], R. S. Getso [a] and Y. I. Bunkure [c]

[a] Department of Physics, Sa'adatu Rimi College of Education Kumbotso, Kano, Nigeria.
[b] Department of Physics, Bayero University, Kano, Nigeria.
[c] Department of Science and Technology Education, Bayero University, Kano, Nigeria.

Authors' contributions

This work was carried out in collaboration among all authors. All authors read and approved the final manuscript.

Article Information

Open Peer Review History:
This journal follows the Advanced Open Peer Review policy. Identity of the Reviewers, Editor(s) and additional Reviewers, peer review comments, different versions of the manuscript, comments of the editors, etc are available here: https://www.sdiarticle5.com/review-history/95374

Original Research Article

Received: 20/10/2022
Accepted: 28/12/2022
Published: 29/12/2022

ABSTRACT

Zinc oxide (ZnO) nano particles were prepared using sol-gel auto combustion method from Zinc acetate dehydrate and sodium hydroxide. Their structural, morphological, optical and electrical properties were studied. X-ray diffraction (XRD) analysis revealed the film's hexagonal wurtzite phase with preferred (101) grain orientation. The mean crystallite size calculated using the Debye-Scherrer model was 23nm with lattice parameters a=0.3255nm and c=0.5185nm (CF. JCPDS 361451) and small dislocation density of 1.8 x 10^{-3}nm^{-2}, which shows the presence of few lattice defects and very good crystallinity. Scanning electron microscope (SEM) micrographs revealed the film granular porous structure composed of collections of hexagonal columnar grains in a direction normal to the substrate surface and an average grain size of around 198.86nm. The UV-Vis room

**Corresponding author: Email: sabuwalle@gmail.com;*

temperature optical absorption coefficient was analysed using the transmission spectra data and the optical band gap energy was estimated to be around 3.3eV. A low electrical resistivity value of $2.35x10^{-4}\Omega m$ was obtained and a high value of carrier charge mobility was found to be $185cmV^{-1}S^{-1}$. The results of this work are important for applications in semiconductor devices particularly solar cells, optical sources and detectors.

Keywords: Zinc oxide; Sol-gel; ZnO; XRD; SEM.

1. INTRODUCTION

"In the past few decades, there has been a paradigm shift in the area of transparent conducting oxide (TCO) thin film research due to their wide use in optoelectronic devices such as touch screen, liquid crystal display, solar cells and light emitting diodes" [1]. "TCOs should demonstrate both high electrical conductivity and high optical transparency in the visible region. Indium tin oxide (ITO) is the most widely due to its high transparency to visible light and high electrical conductivity" [2,3]. "However, there has been a major challenge to find an alternative to ITO because of it high cost, toxicity and scarcity of Indium, which is the principal constituent element of ITO" [2,3]. "The electrical and optical properties of ITO are degraded when exposed to hydrogen plasma environment. To this end, transparent conducting zinc oxide (ZnO) is an attractive substitute material for ITO because of its good optical and electrical properties together with the low cost, non-toxicity and abundance in nature of Zn" [4]. "ZnO is an n-type semiconductor material with a wide band gap of 3.3eV and is employed in a variety of applications including electronic devices, biomedical field ad variety of sensors" (Koklekar et al. 2011). "ZnO has large exciton binding energy (60meV) at room temperature" [5]. "Furthermore, it has high electromagnetical stability, high thermal stability and good stability in hydrogen plasma, compared to ITO" (3, 8, 9, 10, 11). "Due to the good electrical stability of the ZnO thin film it has been previously and presen.tly used in organic light emitting diodes [OLEDs]" (12,13,14).

"The sol–gel auto combustion method is a preferred approach for generating ZnO nanoparticles because of its low cost, dependability, reproducibility, simplicity, and comparatively mild synthesis conditions. Furthermore, the nanoparticles made this way have good optical properties, and the morphology of the particles may be modified by varying the relative rates of hydrolysis and condensation reactions. Controlling these reaction rates, on the other hand, can be problematic". Lee and colleagues, [6]. According to Byung-ki and coworkers, "allowing ammonium carbonate to react with zinc nitrate hydrate produced large surface area ZnO" [7]. "Wong and colleagues reported the formation of ZnO particles from zinc acetate with NaOH in 2-propanol at 0°C and 65°C" [8]. "Tokumoto and co-workers reported that the products obtained from an ethanolic zinc acetate solution using the sol–gel route depend on catalysts and the temperature of hydrolysis. Unwashed nanoparticulate powders were found to be a mixture of ZnO (Wurtzite), zinc acetate, and zinc hydroxy double salts (Zn-HDS)" [9]. "Use of ethanol as solvent for preparing ZnO nanoparticles by the reaction of zinc acetate and sodium hydroxide in an ice bath was also reported by Peng and co-workers" [10]. Santilli and colleagues, on the other hand, pointed out that "the powders recovered from ethanolic zinc acetate sol–gel suspensions were a combination of nanometer-sized zinc oxide (ZnO) and zinc acetate dihydrate ($Zn(CH_3COO)_2.2H_2O$) [11-13]. The order in which these phases formed was unclear" [14]. In this study, a simple sol-gel autocombustion approach was used to synthesize nanostructured ZnO from zinc acetate dihydrate in water with NaOH. The structural, morphological, optical and electrical features of the ZnO metal oxide nano particles obtained were investigated.

2. THEORETICAL BACKGROUND

The mean crystallite size (D) using the Debye-Scherrer formula is given by Verka et al. [15].

$$D = \frac{0.9\lambda}{\beta \cos\theta} \quad (1)$$

where λ, β, θ are the x-ray wavelength (1.541Å), full width at half maximum (FWHM) in radius (corrected for instrumental broadening) and Bragg's diffraction angle respectively.

The dislocation density σ is given by the equation [16].

$$\sigma = \frac{1}{D^2} \quad (2)$$

where D is the mean crystallite size.

The lattice parameters a and c can be calculated [17] using equation

$$\frac{1}{d_{hkl}^2} = \frac{4}{3}\left(\frac{h^2+hk+k^2}{a^2}\right) + \frac{l^2}{c^2} \quad (3)$$

where d_{hkl} is the inter planner spacing obtained from Bragg's law, and h, k and l are the miller indices denoting the plane.

The Zn-O bond length (L) is given by the equation

$$\mathrm{L} = \sqrt{\left(\frac{\mathrm{a}^2}{3} + \left(\frac{1}{2} - \mathrm{u}\right)^{\,2}\mathrm{C}^2\right)} \quad (4)$$

$$\text{and } U = \frac{a^2}{3C^2} + \frac{1}{4} \quad (5)$$

where u is the wurtzite structure parameter. The optical band gap (E_g) can be estimated using the Tauc model in the absorption region, given in equation [4].

$$(\alpha hv)^{\,2} = B\left(hv - E_g\right) \quad (6)$$

where hv is the energy of the incident photon and B is an energy-Independent constant. Eg can be found from the Tauc plot of $(\boldsymbol{\alpha hv})^{\,\mathbf{2}}$ versus hv by extrapolating the linear portion of the absorption edge to $(\boldsymbol{\alpha hv}) = \mathbf{0}$. And $\boldsymbol{\alpha}$ is the optical absorption coefficient which can be calculated in the strong absorption region using Beer-Lambert law in equation (7).

$$\alpha = 2.303\,\frac{A}{d} \quad (7)$$

[18,19].

where d and A are the film thickness and Absorbance respectively.

The electrical resistivity (ρ) from the four-point probe method is given by the equation

$$\rho = 4.532\left(\frac{V}{I}\right)t = R_s t \quad (8)$$

where V, I, R_s and t are the voltages, current, sheet resistance and film thickness respectively. Sheet resistance is given by the equation

$$R_s = \frac{\rho}{t} \quad (9)$$

The hall voltage can be calculated from the equation [20],

$$V_H = \frac{BI}{nqd} = \frac{R_H BI}{d} \quad (10)$$

Where d is the thickness of the sample, q is the charge and n is the charge carrier concentration. The quantity R_H is called Hall coefficient and is given as

$$R_H = \frac{1}{nq} \quad (11)$$

A plot of Hall voltage (V_H) as a function of magnetic field (B) at constant current will have a slope given by

$$slope = \frac{R_H I}{d} \; or \; R_H = \frac{(slope)d}{I} \quad (12)$$

We can measure the carrier concentration according to the relation [21].

$$n_H = \mp\frac{1}{R_H e} \quad (13)$$

Knowing the Hall voltage of the material, the carrier mobility can be calculated from

$$\mu_H = \frac{V_H d}{BI\rho} \quad (14)$$

Where, $V_H$is Hall voltage, d is the thickness, B is the magnetic field strength, I is current and ρ is resistivity.

3. EXPERIMENTAL PROCEDURE

Zinc Oxide nanostructure was synthesized by using sol-gel method at room temperature. In order to prepare a sol, weighing balance was used to weigh 2 g of Zinc Acetate Dihydrate ($Zn(CH_3COO)_2.2H_2O$)., and 8 g of Sodium Hydroxide (NaOH), in stoichiometric ratios and then dissolved in 25 ml of distilled water respectively, and stirred with a constant magnetic stirrer. Then, 100 ml of ethanol dropwise was added to the solution containing both sodium hydroxide and zinc acetate, 9 gm of Polyvinyl pyrrolidone (PVP k-30, M.W -40000 LOBA Chemie) was added to serve as the chelating agent. All the starting materials were used without further purification, the solution was continuously stirred and heated at a temperature of 80-100 ° C until the water evaporated completely by forming a brown gel. To obtain the precursor, the acquired brown gel was placed on a hot plate and cooked for three hours at a

temperature between 280 and 300 ° C. The precursor material was subsequently calcined for four hours at a temperature of 600 ° C. Film Thickness was measured using a 2D surface profilometer (Alpha-step 0-100, KLA-Tencor, USA). Structural properties were examined by an X-ray diffraction system operated at 40kv and 40mA using Cu=kα radiation $\lambda =$ 1.5418Å collected at 20-80^{o} phase size 0.01^{o}. Bruker AXSD8 advanced diffractometer.

The surface morphology was characterized by scanning electron microscope (SEM) operating at 2.00kv. Optical transmittance measurements were performed suing a UV/VIS/NIR spectrophotometer, (Perkin-Elmer, America). In the 250-700nm wavelength range. Electrical properties were evaluated from the current-voltage (I-V) characteristics measurements using the four-point probe equipment. The charge carrier mobility of the ZnO was also determined using Hall effect.

4. RESULTS AND DISCUSSION

4.1 Structural Properties

Fig. 1 shows the XRD pattern of the deposited ZnO thin films. All the diffraction peaks were indexed to ZnO with hexagonal wurtzite crystal structure. The appearance of weak diffraction peaks corresponding to the (200), (004) and (202) planes of ZnO suggested the presence of some randomly oriented grains. There was a strong ZnO peak along (101) plane at $2\theta =$36.20 indicating that the films grow perpendicular to the substrate. This is in good agreement with the findings of Verka et al. [15].

Using the Debye-Scherrer formula presented in equation (1), the mean crystallite size (D) was determined to be 23 nm based on the broadening of the greatest intensity peak corresponding to the (101) diffraction plane. The dislocation density (σ) was calculated from D using equation (2) and was found to be 1.8x10^{-3}nm^{-2}. This is in good agreement with the findings of Muchuweni et al. [4], were they got "a dislocation density (σ) of 1.7x10^{-3}nm^{-2}. This lower value for sigma implies that the film has very few lattice defects and good crystalline qualities". The lattice parameters a and c were calculated using equation (3) and was found to be 3.25Å (0.3259nm) and 5.18Å (0.5185nm) (CF. JCPDS 361451) respectively. The results were in good agreement with the findings of Muchuweni et al. [4]; Kayamata, [22]. The wurtzite structure parameter (U) was calculated using equation (5) and was found to be 0.381. The Zn-O bond length (L) was calculated using equation (4) and was found to be L=1.97Å, which is in good agreement with the findings of Muchuweni et al. [4], were they got a bond length (L) of 1.9767 Å.

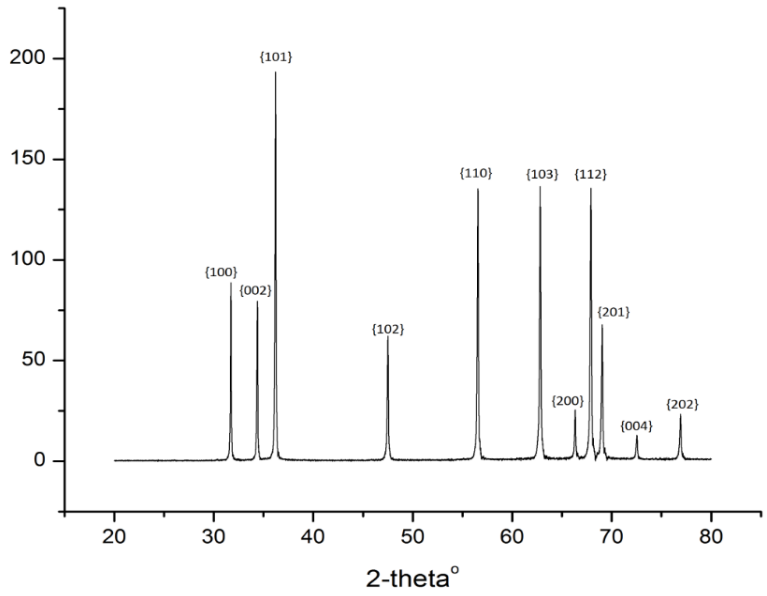

Fig. 1. X-ray Diffractogram of Zincite ZnO

Fig. 2a. SEM micrograph of ZnO annealed at a temperature of 600^{o}C for 1 hour

Fig. 2b. SEM micrograph of ZnO annealed at a temperature of 600^{o}C for 2 hours

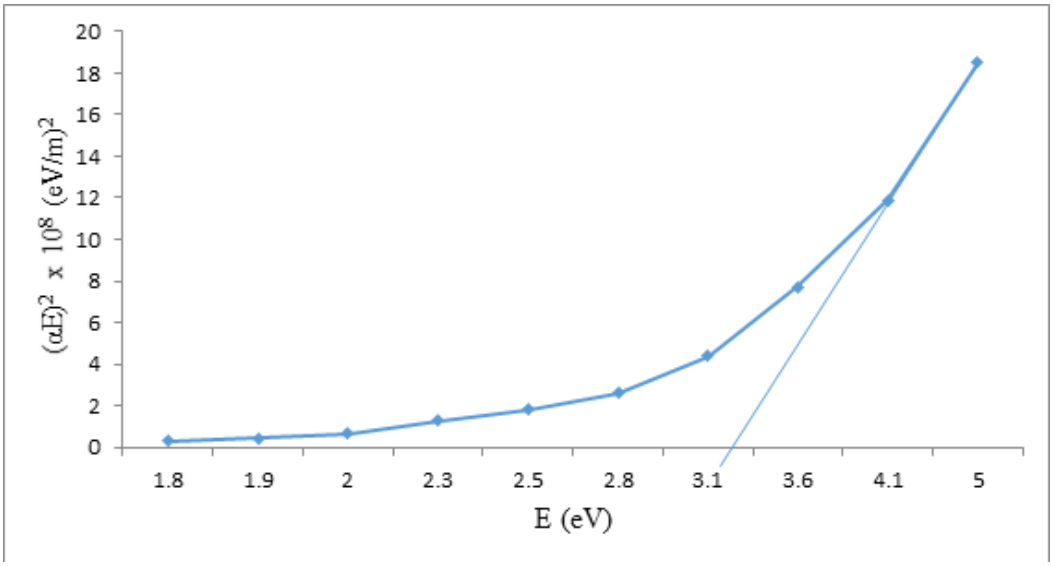

Fig. 3. Graphical determination of the optical band gap energy for ZnO

4.2 Morphological Characteristics

Figs. 2a and 2b show SEM micrographs that were taken for ZnO samples annealed at 600^{o}C for a time of 1hour and 2hours respectively. All the samples had a uniform crack free structure. They also revealed granular porous structure. The ZnO Layer contains a collection of hexagonal columnar grains grown in a direction normal to the substrate surface. It was observed that the sample annealed for two hours is more homogenous, dense and crack free than the sample annealed for 1 hour. Thus, at an extended annealing time, a greater rate of vaporization occurred from the grown crystal and the crystal growth that occurred during the annealing process and crystallite formation in the form of small grains. The average grain size was estimated to be around 198.86nm. The finding is in good agreement with the work of Bouachiba et al. [23] and Izaki et al. [24] where they got a grain size 200nm.

4.3 Optical Properties

The Tauck's plot of the UV-Vis spectra graph of $(\alpha h\nu)^2$ versus $(h\nu)$, shown in Fig. 3 was plotted for ZnO thin film. By extrapolating the linear portion of the absorption edge to $(\alpha h\nu)$=0, the energy band gap was found to be 3.3eV. The result was in concord with previous results of [22,23,25] were they got 3.3eV, 3.28eV and 3.23 respectively.

4.4 Electrical Properties

Fig. 4 shows the current and corresponding voltages measured through the grown ZnO crystals annealed at a temperature of 600^{o}C for a period of 2 hours. The resistivity of the sample was calculated using equation (8) as 2.35x10^{-4}Ωm. The result is in concord with the findings of Getso, (2016) where he got 2.37x10^{-4} Ωm. The result is slightly lower because the electrical resistivity of the thin films may be affected by

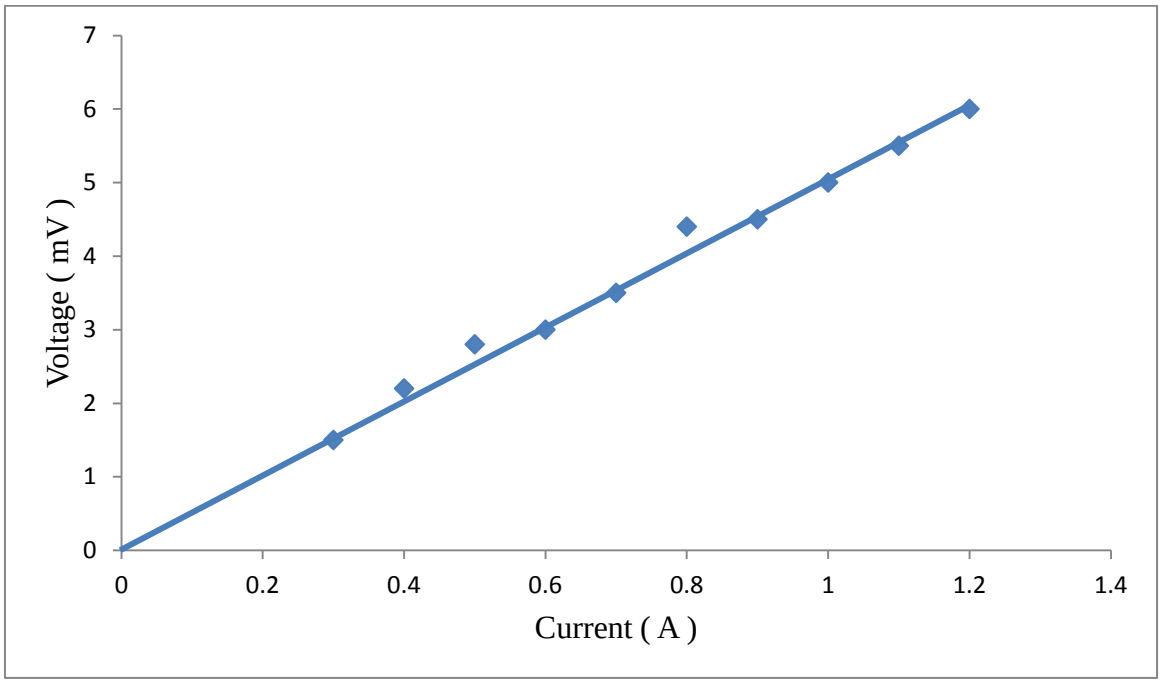

Fig. 4. Current- voltage graph from the four-point probe experiment of ZnO

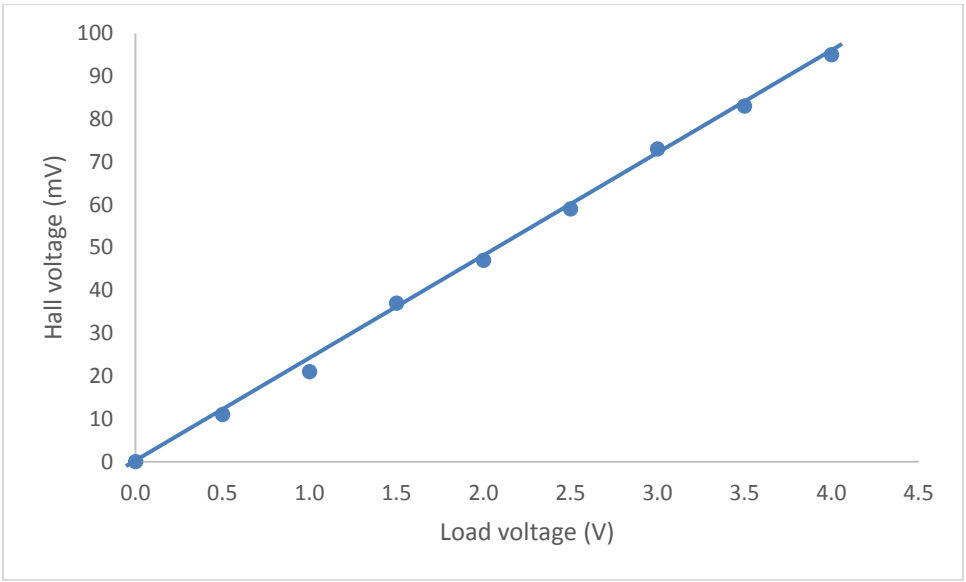

Fig. 5. V_H-V_L graph of the synthesized ZnO crystal

isotropic background scattering (arising from photons and point defects). Similarly, the charge carrier mobility was calculated using equation (14) and was found to be $185cm^2/V^{-1}S^{-1}$, the result agrees with the findings of Mitali et al. (2015) where they got $183.7cm^2/V^{-1}S^{-1}$.

5. CONCLUSION

The structural, morphological, optical and electrical properties of ZnO thin film were characterized. The film had a hexagonal wurtzite crystal structure with the preferred orientation along the (101) direction. The mean crystallite size was found to be 23nm and the lattice parameters were found to be a=0.3255nm and c=0.5185nm and small dislocation density of $1.8x10^{-3}nm^{-2}$. SEM micrograph showed film granular porous structure composed of collection of hexagonal columnar grains with an average grain size of 198.86nm. The optical band gap

was found to be 3.3eV. A low electrical resistivity of $2.72x10^{-4}\Omega m$ indicated the suitability of the ZnO thin film for optoelectronic application.

COMPETING INTERESTS

Authors have declared that no competing interests exist.

REFERENCES

1. Muchuweni E, Sathiaraj TS, Nyakotyo H. Effect of gallium doping on the structural optical and electrical properties of zinc oxide thin films prepared by spray pyrolysis. Ceramics International. 2016; 42(8):10066–10070.
2. Sathiaraj TS. Effect of annealing on the structural optical and electrical properties of ITO films by RF sputtering under low vacuum level. Microelectronics Journal. 2008;39(12):1444–1451. DOI:https://doi.org/10.1016/J.MEJO.2008.06.081
3. Zhang Y, Duan L, - al Lin W.-X, Wang J.-F, Li Q, Kumar Srivastava A, Kumar J. Effect of zinc addition and vacuum annealing time on the properties of spin-coated low-cost transparent conducting 1 at% Ga–ZnO thin films. Science and Technology of Advanced Materials. 2013;14(6):065002. DOI:https://doi.org/10.1088/1468-6996/14/6/065002
4. Muchuweni E, Sathiaraj TS, Nyakotyo H. Physical properties of gallium and aluminium co-doped zinc oxide thin films deposited at different radio frequency magnetron sputtering power. Ceramics International. 2016;42(15):17706–17710. DOI:https://doi.org/10.1016/J.CERAMINT.2016.08.091
5. Shinde SS, Shinde PS, Oh YW, Haranath D, Bhosale CH, Rajpure KY. Structural optoelectronic luminescence and thermal properties of Ga-doped zinc oxide thin films. Applied Surface Science. 2012;258(24):9969–9976. DOI:https://doi.org/10.1016/J.APSUSC.2012.06.058
6. Lee JA, Easteal J, Pal U, Bhattacharyya D. Evolution of ZnO nanostructures in sol–gel synthesis. Current Applied Physics. 2008;9:792–796.
7. Byung-Ki N, Arden A, Walters B, Albert Vannice M. Studies of gas adsorption on ZnO using ESR FTIR spectroscopy and MHE (microwave Hall Effect) measurement. Journal of Catalysis. 1993; 140:585-600.
8. Wong EM, Paul G, Hoertz Cindy J, Liang Bai-Ming Shi Gerald J. Meyer, Peter C. Searson. Influence of organic capping ligands on the growth kinetics of ZnO nanoparticles. Langmuir. 2001;17:8362-8367.
9. Tokumoto MS, Sandra H. Pulcinelli Celso V. Santilli, Vale´rie Briois. Catalysis and temperature dependence on the formation of ZnO nanoparticles and of zinc acetate derivatives prepared by the sol-gel route. J. Phys. Chem. B. 2003;107:568-574.
10. Peng WQ, Qu SC, Cong GW, Wang ZG. Structure and visible luminescence of ZnO nanoparticles. Materials Science in Semiconductor Processing. 2006;9:156–159.
11. Rao TP, Kumar MCS. Physical properties of Ga-doped ZnO thin films by spray pyrolysis. J. Alloy. Compd. 2010;506:788–793.
12. Rao TP, Kumar MCS. Resistivity stability of Ga Doped ZnO thin films with heat treatment in air and oxygen atmospheres. J. Cryst. Process Technol. 2012;2:72–79.
13. Kolekar TV, Yadav HM, Bandgar SS, Deshmukh PY. Synthesis by sol-gel method and characterization of Zno nanoparticles. Indian Streams Research Journal. ISSN 2230-7850. 2011;1(1)
14. Santilli CV, Pulcinelli SH, Tokumoto MS, Briois V. In situ UV–vis and EXAFS studies of ZnO quantum-sized nanocrystals and Zn-HDS formations from sol–gel route. Journal of the European Ceramic Society. 2007;27:3691–3695.
15. Verka G, Atanas T, Mariana G. Low cost solar cells based on cuprous oxide Solar cells-Thin film technologies Prof. Leonid A. Kosyachenko (Ed.):InTech Croatia. 2011;55-76.
16. Wang XS, Wu ZC, Webb JF, Liu ZG. Ferroelectric and dielectric properties of Li-doped ZnO thin films prepared by pulsed laser deposition Appl. Phys. A. 2003; 77:561–565.
17. Prieur D, Bonani W, Popa K, Walter O, Kriegsman KW, Engelhard MH, Guo X, Eloirdi R, Gouder T, Beck A, Vitova T, Scheinost AC, Kvashnina K, Martin PSize Dependence of Lattice Parameter and Electronic Structure in CeO2 Nanoparticles. Inorganic Chemistry. 2020; 59(8):5760–5767.

18. Sandcep S, Dhananjaya K. Effect of annealing temperature on the structure and optical properties of zinc oxide (ZnO) thin film prepared by spin coating process. Department of sciences Manipal University. 576 10k Karnataka India. International Conference on Material Science and Technology (ICMST); 2012.
19. Mohammad AT, Darma TH. Barde A, Isyaku S, Umar AH. Investigation of the morphology and optical properties of $CuAlO_2$ thin film. Journal of Applied and Physical Sciences. 2017;3 (1):17-25.
20. Abas A, Halim SA, Talib ZA, Wahab ZA. A simple automated system for hall effect measurements. Sains Malysiana. 2012;41(4):611-615
21. Hassan BK, Abdulhassan SK, Mustapha. Electrical conductivity and hall effect measurements of ($CuInTe_2$) Thin Films Ibn-Al-Haitham Journal for Pure and Applied Science. 2016;29(2).
22. Katayama JK, Ito MM, Tamaki J. Performance of Cu_2O/ZnO solar cell prepared by two-step electrodeposition. Journal of Applied Electrochemistry. 2004;36:687-692.
23. Bouachiba Y, Mammeri A, Bouabellou A, Rabia O, Saidi S, Taabouche A, Rahal B, Benharrat L, Serrar H, Boudissa M. Optoelectronic and birefringence properties of weakly Mg-doped ZnO thin films prepared by spray pyrolysis. Journal of Materials Science: Materials in Electronics. 2022;33(9):6689–6699. DOI:https://doi.org/10.1007/S10854-022-07844-3/METRICS
24. Izaki M, Shinagawa T, Mizuno K, Ida Y, Inaba M, Tasaka A. Electrochemically constructed p-Cu_2O / n-ZnO heterojunction diode for photovoltaic device. J. phys. D: Appl. Phys. 2007;40:3326-3329.
25. Ream SK, Mustafa SH, Sameer GM. Synthesis of ZnO thin film by chemical spray pyrolysis using its nano powder. Kuwait Journal of Science. 2022;49(1):1-11.

Peer-review history:
The peer review history for this paper can be accessed here:
https://www.sdiarticle5.com/review-history/95374